IVYSPRING INTERNATIONAL PUBLISHER

*International Journal of Biological Sciences*

2017; 13(10): 1287-1296. doi: 10.7150/ijbs.18890

Research Paper

# Exosomal miR-7 Mediates Bystander Autophagy in Lung after Focal Brain Irradiation in Mice

Shang Cai[1, 2*], Geng-Sheng Shi[3*], Hui-Ying Cheng[2, 4], Ya-Nan Zeng[2, 4], Gen Li[2, 4], Meng Zhang[2, 4], Man Song[2, 4], Ping-Kun Zhou[2], Ye Tian[1, 2], Feng-Mei Cui[2, 4]✉, Qiu Chen[2, 4]✉

1. Department of Radiotherapy and Oncology, The Second Affiliated Hospital of Soochow University, Suzhou 215004, P R China;
2. Collaborative Innovation Center of Radiation Medicine of Jiangsu Higher Education Institutions, Suzhou 215123, P R China;
3. Shandong Academy of Occupational Health and Occupational Medicine, Shandong Academy of Medical Sciences, Jinan 250062, P R China;
4. Department of Radiation Medicine, School of Radiation Medicine and Protection, Medical College of Soochow University, Suzhou 215123, P R China.

* These authors have contributed equally to this work.

✉ Corresponding authors: Feng-mei Cui or Qiu Chen, Department of Radiation Medicine, School of Radiation Medicine and Protection, Medical College of Soochow University, Suzhou 215123, China; telephone (512)65880068; fax (512)65880052; E-mail: cuifengmei@suda.edu.cn or happyqiu@suda.edu.cn



Received: 2016.12.23; Accepted: 2017.08.04; Published: 2017.09.21

## Abstract

This study investigated whether exosomal microRNA-7 (miR-7) mediates lung bystander autophagy after focal brain irradiation in mice. After 10 Gy or sham irradiation of mice brains, lung tissues were extracted for the detection of autophagy markers by immunohistochemistry, western blotting, and quantitative real-time reverse transcription PCR (qRT-PCR), meanwhile the brains were dissociated, the neuron/astrocyte/microglia/oligodendrocyte were isolated, and the miR-7 expression in each population were detected, respectively. A dual-luciferase reporter assay was developed to identify whether *Bcl-2* is a target gene of miR-7. After 10 Gy or sham irradiation of astrocytes, exosomes were extracted, stained with Dil (1,1'-Dioctadecyl-3,3,3',3'-Tetramethylindocarbocyanine Perchlorate), and added into non-irradiated astrocytes. Meanwhile, Dil-stained exosomes released from 10 Gy or sham irradiated astrocytes were injected into LC3B-GFP mice via the tail vein. Lung tissues were then extracted for western blotting and qRT-PCR. Irradiation of mouse brains increased the LC3B-II/I ratio, Beclin-1 and miR-7 levels, while decreased the Bcl-2 level in non-irradiated lung tissue. Interestingly, brain irradiation remarkably increased the miR-7 expression in astrocyte and oligodendrocyte. MiR-7 significantly inhibited the luciferase activity of the wild-type *Bcl-2*-3′-untranslated regions (UTR) reporter vector, but not that of the *Bcl-2*-3′-UTR mutant vector, indicating that *Bcl-2* is directly targeted by miR-7. In *in vitro* study, the addition of irradiated astrocyte-secreted exosomes increased the LC3B-II/I ratio, Beclin-1 and miR-7 levels, while decreased the Bcl-2 level in non-irradiated astrocytes. Further, the injection of irradiated astrocyte-secreted exosomes through the tail vein increased the lung LC3B-II/I ratio, Beclin-1 and miR-7 level, but decreased the Bcl-2 level *in vivo*. We concluded that exosomal miR-7 targets *Bcl-2* to mediate distant bystander autophagy in the lungs after brain irradiation.

Key words: exosome, miR-7, radiation, radiation induced bystander effect (RIBE), autophagy.

## Introduction

About two-thirds of all tumor patients will receive radiotherapy (RT) during the course of their treatment [1]. However, protecting normal tissues from RT-induced injury still remains a challenge. Ionizing radiation (IR) can induce biological effects, including genomic instability, cell cycle arrest, gene mutation, and even carcinogenesis in non-irradiated cells [2, 3], which is termed the radiation induced bystander effect (RIBE). Although a growing number of studies have focused on RIBE both *in vitro* and *in vivo* [4-6], it still remains a poorly understood issue. Thus, determining the detrimental effects of RIBE, especially distant RIBE, and its underlying molecular mechanism is vital for RT.

Autophagy can be activated by various stimuli, including IR [7-9]. A recent study demonstrated

activation of autophagy in non-irradiated bystander cells that were cultured in conditioned medium (CM) collected from irradiated cells [9], indicating that autophagy may be one of the research endpoints for RIBE.

Exosomes are small membrane-bound vesicles containing microRNAs (miRNAs), DNAs, mRNAs, proteins, and soluble factors [10-13]. Recent studies have indicated the involvement of exosomes in IR-related communications between cells [6, 14, 15]. MiRNAs modulate gene expression by binding to the 3′-untranslated regions (UTRs) of target genes [16-18] , and play critical roles in several biological and pathological processes, including carcinogenesis and autophagy [19, 20]. Several studies have identified a role for miRNAs in cellular responses to RIBE [21-23]. Our recently published paper showed that miR-7-5p mediates RIBE *in vitro* [6]: we have identified a set of differentially expressed miRNAs in the exosomes collected from 2 Gy irradiated human bronchial epithelial BEP2D cells, from which miR-7-5p was found to induce autophagy in recipient cells. The data showed that the exosomes-containing miR-7-5p is a crucial mediator of bystander autophagy. Taken together, exosomes and inside miRNAs including miR-7 might serve as the major regulators of distant RIBE.

In this study, we hypothesized that exosomes transfer IR-induced signals from irradiated cells to distant non-irradiated bystander cells via miRNAs, which consequently trigger and regulate RIBE. Our data identified that focal brain IR induced autophagy in non-irradiated lungs *in vivo*, and confirmed that exosomal miR-7 mediates the bystander effect of autophagy in lungs induced by brain irradiation via targeting *Bcl-2* both *in vivo* and *in vitro*.

## Materials and Methods

### Animals

All animal handling procedures were reviewed and approved by the Animal Care/User Ethical Committee of Soochow University, Suzhou City, P. R. China. C57BL/6 mice and LC3B-GFP transgenic mice (6–8 weeks old, weighing 16–22 g, 50% males and 50% females) were purchased from the Model Animal Research Center of Nanjing University (Nanjing, China). All animals were maintained in a specific pathogen free (SPF)-grade facility of Soochow University under controlled conditions. The experimental procedures for all mice were performed in accordance with the Regulations for the Administration of Affairs Concerning Experimental Animals approved by the State Council of People's Republic of China.

### Irradiation

C57BL/6 mice and LC3B-GFP transgenic mice were subjected to X-ray irradiation using an SL18 linear accelerator (Siemens, Germany) at the Department of Radiotherapy and Oncology, Suzhou Kowloon Hospital (n = 6 mice in each group). The heads of mice were exposed to 10Gy irradiation delivered at 200 cGy/min. Astrocytes were exposed to 10Gy irradiation delivered at 1.2 Gy/min using an X-ray radiometer (Radsource) at Jiangsu Province Key Laboratory of Radiation Medicine and Prevention.

### Isolation of neuron/astrocyte/microglia/oligo-dendrocyte

2 hours after brain irradiation, mice were anesthetized and decapitated. The scalp and the entire dorsal portion of the cranium were removed. The meninges and pia mater were stripped free and discarded. The whole brain were mechanically dissociated by gentleMACS™ Dissociator (catalog number 130093235, program brain 03) in C tubes. Isolation of neuron/astrocyte/microglia/ oligodendrocyte populations were performed following tissue dissociation using protocols from Miltenyi Biotec's Neuronal Isolation Kit (catalog number 130098752), Anti-ACSA-2 kit (catalog number 130097678), $CD11b^+$ and O4 Microbeads (catalog number 130093634 and 130094543). Neurons were negatively selected but others were positively selected. Cells were collected and total RNA was extracted. Then the relative expression of miR-7 was detected by qRT-PCR.

### Isolation and culture of primary astrocytes

Primary astrocytes were isolated from mice that were less than 2 days old. The brain cells were harvested and filtered. Cells at a density of $5 \times 10^5/cm^2$ were seeded in flasks and cultured at 37 °C for 2 h. During this process, fibroblasts were identified and removed according to their different adherence ability. The cell suspension was re-seeded in flasks coated in poly-L-lysine (0.1 mg/mL) and cultured for three days. The medium was changed four times and the cells were divided in two fractions: microglial cells (upper) and astrocytes (lower). Microglial cells were removed according to their poor adherence ability. The astrocytes were cultured and prepared for next experiments.

### Dual-luciferase reporter assay

The miR-7 mimics and inhibitors were purchased from Shanghai GenePharma Company (GenePharma, Shanghai, China). The miR-7 mimics and inhibitors were transfected into cells using lipofectamine 2000 (Invitrogen, Carlsbad, CA, USA) in

six-well plates according to the manufacturer's instructions.

The pmirGLO-Bcl-2-3′-UTR plasmid was identified by double digestion and agarose gel electrophoresis. A QuikChange Site-Directed Mutagenesis Kit (Agilent Technologies, Santa Clara, CA, USA, D200514) was used to create the indicated mutations.

The wild-type or mutant vectors were transfected into HEK 293T cells using lipofectamine 2000 in six-well plates according to the manufacturer's instructions. The luciferase activity was measured using a Dual-Glo® Luciferase kit according to the manufacturer's protocol. The activities of firefly luciferase and Renilla luciferase were determined, with the latter used as the internal control.

### Exosome isolation and labeling

Astrocytes were cultured in serum-free medium and exposed to X-ray radiation. Cell supernatants were collected 0, 2, and 6 h after irradiation. Exosomes were isolated from the cell medium by ultracentrifugation (LP-100, Beckman Coulter). Briefly, the cell medium was centrifuged, then supernatants were collected and subjected to gradient centrifugation to remove cell debris. Large vesicles were removed using a 0.22 μm Millex GP syringe filter and exosomes were harvested by ultracentrifugation at 100,000 × *g* for 120 min twice and stored at −80 °C. Exosomes were identified under a transmission electron microscope, re-suspended in PBS, and incubated with Dil dye (Beyotime) at 37°C for 15 min in the dark. After labeling, the exosomes were washed and stored.

### Injection of exosomes into mice

The exosomes secreted from irradiated and non-irradiated astrocytes were re-suspended in PBS and injected separately into mice via the tail vein every three days for a total of five times. Mouse lung tissues were collected 6 h after the last injection.

### Quantitative Real-time Reverse Transcription PCR (qRT-PCR)

Total RNAs from astrocytes and tissues were extracted using the TRIzol® reagent and quantified using a Nanodrop 2000 c (ThermoFisher Scientific). Complementary DNA (cDNA) was generated from 1 μg of total RNA using an RTase M-MLV kit (Takara).

For qRT-PCR, 0.5 μL of the cDNA product was added to a 20 μL reaction volume and gene expression was measured using a Taqman probe real-time PCR assay (Roche, Basel, Switzerland) in the ViiA 7 real-time PCR system (AB applied biosystems). The PCR was conducted according to the manufacturer's protocol.

### Western blotting

Proteins were extracted from cells or tissues and quantified using a BCA assay kit (ThermoFisher Scientific). Thirty micrograms of protein was subjected to SDS-PAGE and then transferred to a polyvinylidene fluoride membrane. The membrane was blocked in 10 % non-fat milk for 60 min and then incubated with primary antibodies at 4 °C overnight. After washing, the membrane was incubated with goat anti-mouse IgG or goat anti-rabbit IgG at room temperature for 60 min. The signals were developed using an ECL detection system.

### Immunohistochemistry

Paraffin-embedded tissues were deparaffinized, followed by rehydration and incubation with 10 % hydrogen peroxide for 15 min. Next, antigen retrieval was performed by microwaving the sections in citric acid solution for 1.5 min. Sections were blocked using 5 % goat serum for 30 min and incubated with antibodies recognizing LC3B, Beclin-1, Bcl-2, or cleaved caspase-3 at 4°C overnight, followed by incubation with the respective secondary antibodies at 37 °C for 30 min. Finally, the sections were developed with diaminobenzidine and detected under a microscope.

### Statistical analysis

Data were analyzed using the SAS 9.3 software. The expression of miR-7 and Bcl-2 was measured using the two-delta cycle threshold (ΔΔCT) method and the difference between two groups was determined using a t-test. For the luciferase activity analysis, the difference between two groups was measured by the Student–Newman–Keuls (SNK) q value. $P < 0.05$ was considered statistically significant.

## Results

### Induction of autophagy in lung after focal brain irradiation in mice

To determine whether brain irradiation could induce autophagy in lung, immunohistochemistry was performed on mouse lung tissue 0, 2, and 6 h after brain irradiation. The number of LC3B and Beclin-1 positive lung cells increased significantly after irradiation (Fig. 1A), while no obvious difference was observed in terms of the amount of cleaved caspase-3 positive cells in the three groups (data not shown), indicating that brain irradiation mainly induced autophagy in lung tissue. To further confirm the induction of autophagy in lung cells, LC3B-GFP transgenic mice were subjected to brain irradiation. Consistently, the amount of LC3B-GFP dots was

significantly higher in lung cells from irradiated mice compared with control group (Fig. 1B). The ratio of LC3B-II/LC3B-I is often used as a marker of autophagy. Western blotting results showed that the ratio of LC3B-II/LC3B-I, and the level of Beclin-1 in lung tissue increased remarkably 6h after irradiation (Fig. 1C). These data indicated that focal brain irradiation induced autophagy in non-irradiated lung tissue.

## Changes of miR-7 and Bcl-2 expressions in the brain, blood, and lung after focal brain irradiation

The results above suggested that focal brain irradiation could induce autophagy in lung cells, and prompted us to investigate the molecular mechanism underlying this distant RIBE. To determine whether lung autophagy is mediated by miR-7, the expressions of miR-7 was quantified by qRT-PCR. The level of miR-7 was significantly increased in mouse lungs 6h after brain irradiation (Fig. 2A). Fig. 2A also showed the dynamic changes of miR-7 expressions in the mouse brain, blood, and lung after irradiation. Interestingly, at the 2h time point, miR-7 in the brain and blood increased significantly, while miR-7 in the lung remained unchanged. At the 6h time point, miR-7 levels in the lung increased remarkably, however, in the brain and blood, miR-7 had returned to normal levels. These data indicated the miR-7 might be released into the blood by the brain upon irradiation and subsequently transferred into the lungs.

*Bcl-2* is an important mediator of autophagy, and our computational analysis showed that *Bcl-2* is one of the target genes of miR-7. Immunohistochemistry results showed that the number of Bcl-2 positive lung cells was dramatically reduced after brain irradiation compared with the control group (Fig. 2B). Further, qRT-PCR result showed that *Bcl-2* mRNA levels in lung tissue were decreased significantly after brain

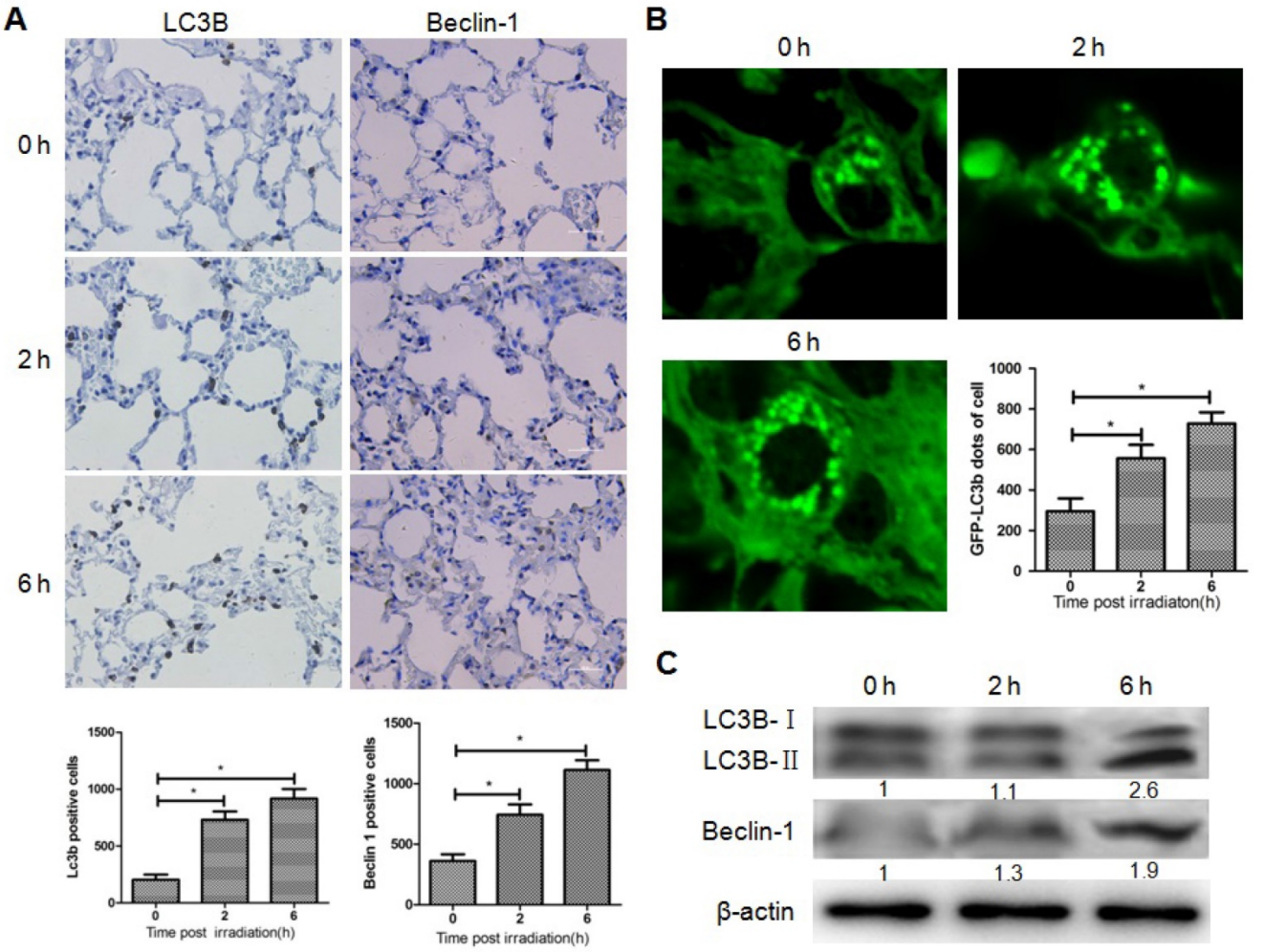


**Figure 1. Brain irradiation induced autophagy in bystander lungs.** Panel A: Lung tissues were obtained 0, 2, and 6 h after 10 Gy brain irradiation, and subjected to immunohistochemistry; LC3-B and Beclin-1 positive cells were quantified. Panel B: Lung tissues from GFP-LC3B transgenic mice were obtained 0, 2, and 6 h after 10 Gy brain irradiation. The number of GFP-LC3 dots was counted in five independent visual fields. Panel C: The expressions of LC3-B and Beclin-1 in lung tissues were measured by western blotting; Thirty micrograms of protein was subjected to do and β-actin was used as internal control. Bars represent the mean ± SD, n=3, * *P* value < 0.05.

irradiation (Fig. 2C). Consistently, western blotting result showed that Bcl-2 protein level in the lung was remarkably decreased 2h and 6h after irradiation (Fig. 2D). These data indicated that focal brain irradiation increased miR-7 expression, while decreased Bcl-2 expression in non-irradiated lung tissues.

## Bcl-2 is a direct target gene of miR-7

The classic dual-luciferase reporter assay was used to identify whether *Bcl-2* was a direct target of miR-7. Bioinformatics analysis using TargetScan showed that the *Bcl-2* 3′-UTR comprises 15 bases that are complementary to miR-7 (Fig. 3A). The optimal concentrations of miR-7 mimics and inhibitor for transfection were then determined (Fig. 3B). Compared with the control, transfection of miR-7 mimics significantly suppressed the luciferase activity of the wild-type Bcl-2-3′-UTR reporter vector, but not that of the mutant Bcl-2-3′-UTR vector. Meanwhile, the transfection of miR-7 inhibitor increased the luciferase activity of wild-type Bcl-2-3′-UTR vector remarkably, but not that of the mutant Bcl-2-3′-UTR vector (Fig. 3C). Next, we measured the *Bcl-2* mRNA level in HEK-293T cells transfected with miR-7 mimics or the inhibitor, and the results showed that the expression of miR-7 correlated negatively with the expression of *Bcl-2* (Fig. 3D). These results indicated that miR-7 regulates *Bcl-2* expression negatively by binding to a specific region in the Bcl-2-3′-UTR sequence.

## Changes of miR-7 expressions in neuron/astrocyte/microglia/oligodendrocyte after focal brain irradiation in mice

The results above proved that irradiation could increase the expression of miR-7 in brain. To determine these miR-7 were derived from which cell population, after 10Gy or sham brain irradiation, neuron/astrocyte/microglia/oligodendrocyte were isolated and subjected to qRT-PCR. The data showed that irradiation significantly increased the miR-7 expression in astrocyte and oligodendrocyte (Fig. 4A, Fig. 4D). These results indicated the miR-7 were mainly derived from astrocyte and oligodendrocyte after brain irradiation.

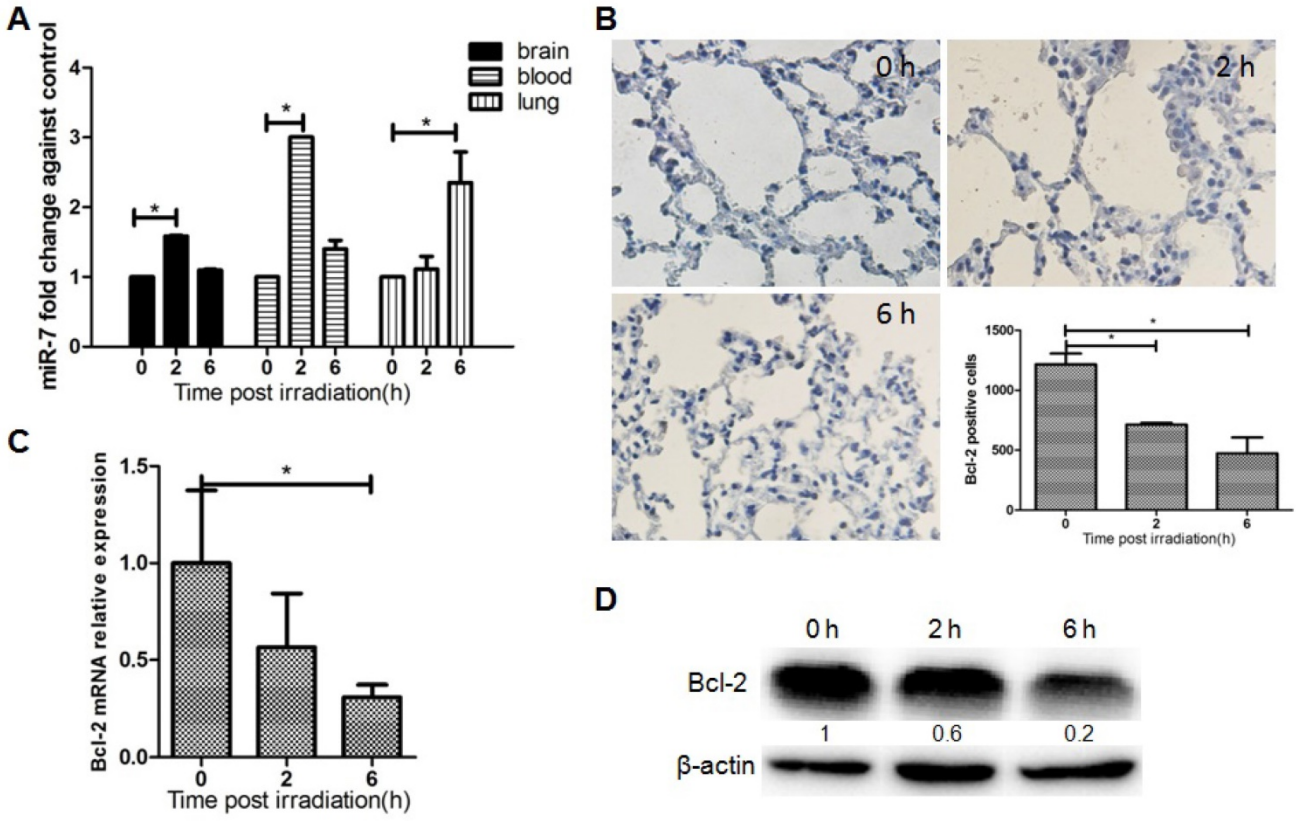


**Figure 2. Brain irradiation increased miR-7 level, while decreased Bcl-2 level in lungs** Panel A: MiR-7 levels in mouse brain, blood, and lung were measured by qRT-PCR at indicated time points after 10 Gy brain irradiation; U6 was used as internal control. Panel B: Mouse lung tissue were obtained and subjected to immunohistochemistry; Bcl-2 positive cells were counted. Panel C: Total RNAs of lung tissue were obtained and subjected to qRT-PCR using a *Bcl-2* specific primer, and 18s rRNA was used as internal control. Panel D: Total proteins of lung tissue were extracted and subjected to western blotting using a Bcl-2 primary antibody, and β-actin as the loading control. Bars represent the mean ± SD, n=3, * *P* value < 0.05.

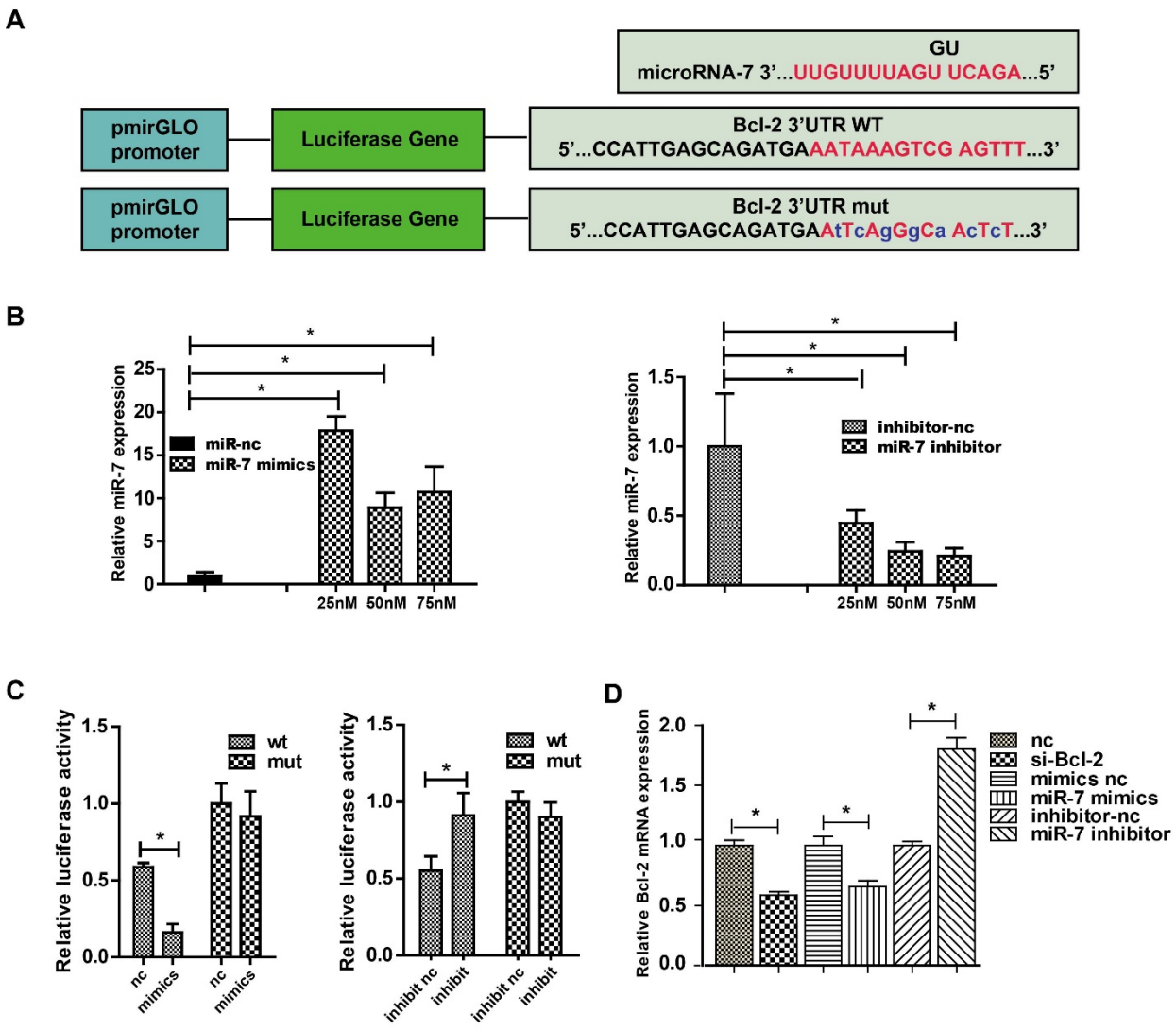


**Figure 3. MiR-7 targets *Bcl-2* directly**. Panel A: Complementary sequences between miR-7 and *Bcl-2* mRNA 3'-UTR (paired bases are marked in red and mutant bases are indicated in blue). Vector pmirGLO was used to construct the expression vector and mutant vector. Panel B: Relative miR-7 expression after treatment with various concentrations of miR-7 mimics or miR-7 inhibitor. Panel C: HEK 293 cells were transfected with wild-type Bcl-2-3'-UTR or mutant Bcl-2-3'-UTR vector together with miR-7 mimics or miR mimics control, or with miR-7 inhibitor or miR inhibitor control, then luciferase activity was measured. Panel D: *Bcl-2* mRNA expression in HEK-293T cells after transfection with Bcl-2 siRNA, miR-7 mimics, or miR-7 inhibitor. 50 nM of miR-7 mimics and 75 nM of miR-7 inhibitor were used. Bars represent the mean ± SD, n=5, * *P* value < 0.05.

## Exosomal miR-7 mediates bystander autophagy in lungs induced by brain irradiation

Based on the results above, we further hypothesized that brain exosomes containing high levels of miR-7 are released into blood upon irradiation. These exosomes then reach the lung tissue through pulmonary capillaries and are internalized by lung cells. Then, the increased levels of miR-7 induce autophagy in lung cells. To confirm this hypothesis, exosomes from the astrocytes of LC3-GFP mice were observed under transmission electron microscope, and exosome biomarkers CD63 and TSG101 were detected (Fig. 5A). 10 Gy irradiation significantly increased the miR-7 level in both astrocytes (Fig. 5B) and astrocytes-secreted exosomes (Fig. 5C) compared with control group. qRT-PCR showed that the internalization of exogenous exosomes from irradiated astrocytes increased the levels of miR-7 and decreased the *Bcl-2* mRNA levels compared with those from non-irradiated astrocytes (Fig. 5D). Consistently, the western blotting results showed that internalization of exogenous exosomes from irradiated astrocytes increased the ratio of LC3B-II/LC3B-I and the Beclin-1 level, while decreased Bcl-2 level compared with those from non-irradiated astrocytes (Fig. 5E).

As expected, Dil-stained exosomes were internalized by astrocytes, and red vesicles, termed endosomes or autophagosomes, were detected in the cytoplasm of astrocytes cultured in medium added with exosomes from 10Gy irradiated astrocytes, but not that from sham irradiated astrocytes (Fig. 6).

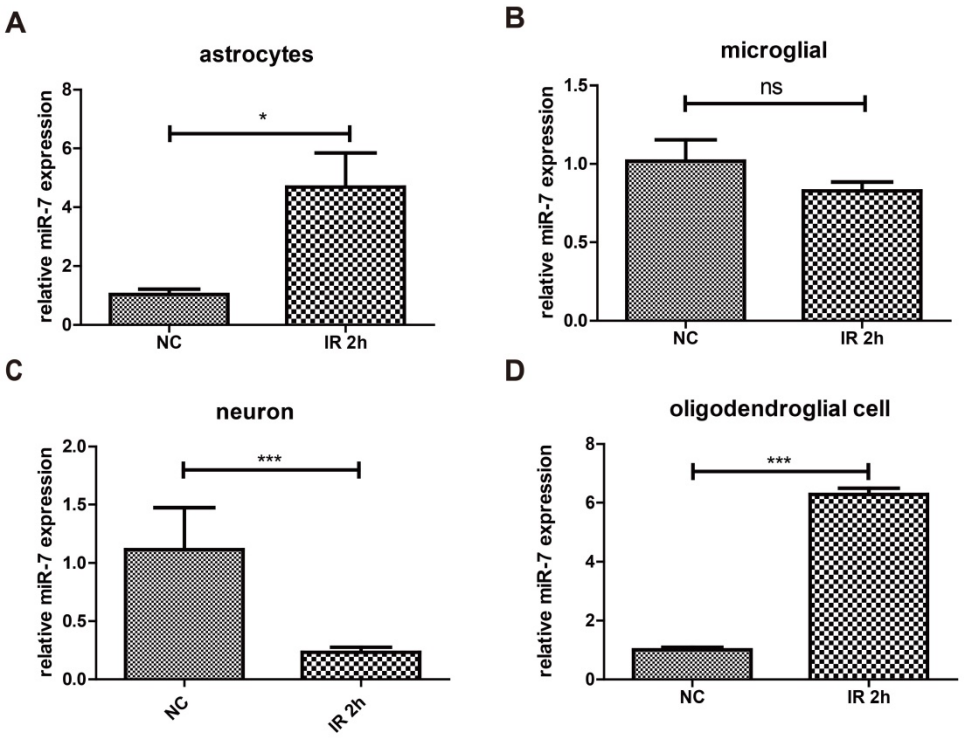


**Figure 4. Brain irradiation increased miR-7 expression in astrocytes and oligodendrocytes, but decreased that in neurons and microglia** After 10Gy or sham brain irradiation, mice brain were obtained, astrocyte, microglia, neuron and oligodendrocyte were isolated. Then the miR-7 expression in these cells were deceted by qRT-PCR (fig.4A to fig.4D), respectively. Bars represent the mean ± SD, n=5, * *P* value < 0.05, *** *P* value < 0.01, NS stands for none significant.

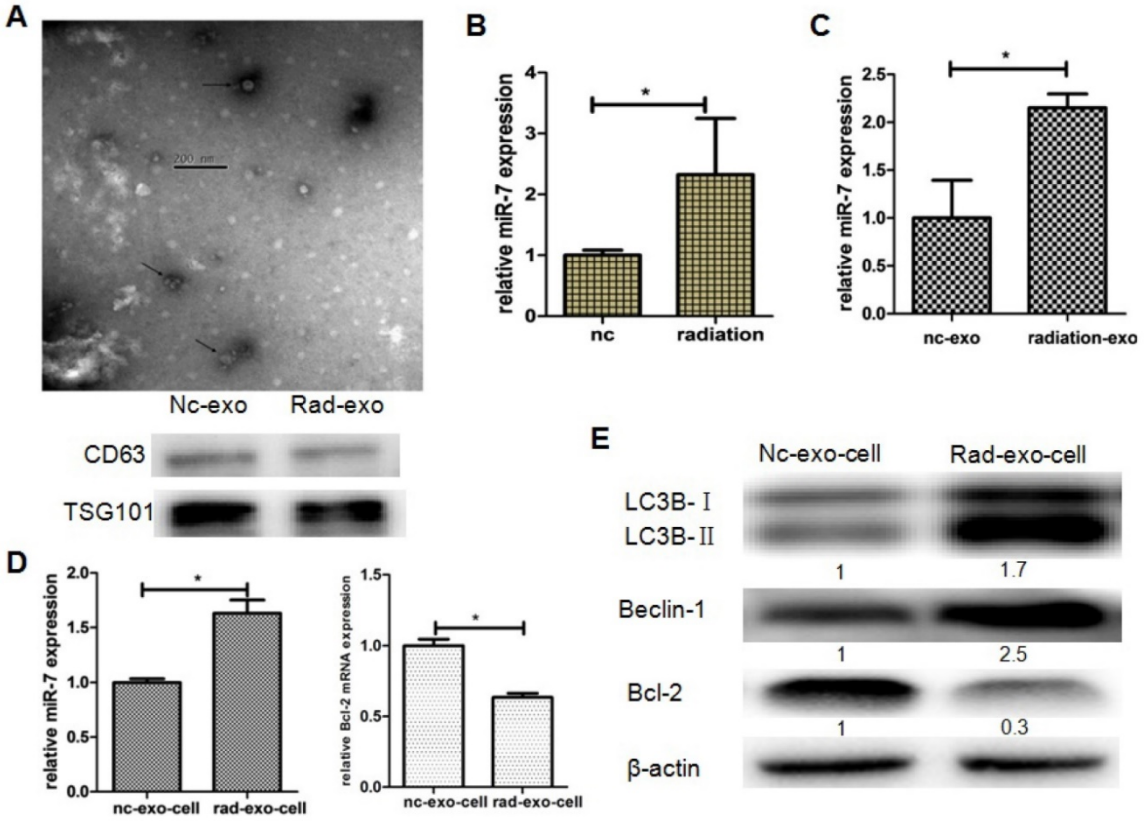


**Figure 5. Exosomal miR-7 mediates bystander autophagy *in vitro*.** Panel A: Exosomes were observed under a transmission electron microscope, while exosomal markers TSG101 and CD63 were measured by western blotting. Panel B: miR-7 levels in astrocytes were measured by qRT-PCR after irradiation; U6 was used as internal control. Panel C: miR-7 levels in exosomes secreted by astrocytes were measured by qRT-PCR after irradiation; U6 was used as internal control. Panel D: Expressions of miR-7 and *Bcl-2* mRNA in irradiated (rad-exo) or non-irradiated (nc-exo) astrocytes-released exosomes were measured by qRT-PCR; U6 was used as internal control. Panel E: Expression of LC3B, Beclin-1, and Bcl-2 in irradiated (rad-exo) or non-irradiated (nc-exo) astrocytes-released exosomes were measured by western blotting after irradiation. Bars represent the mean ± SD, n=5, * *P* value < 0.05.

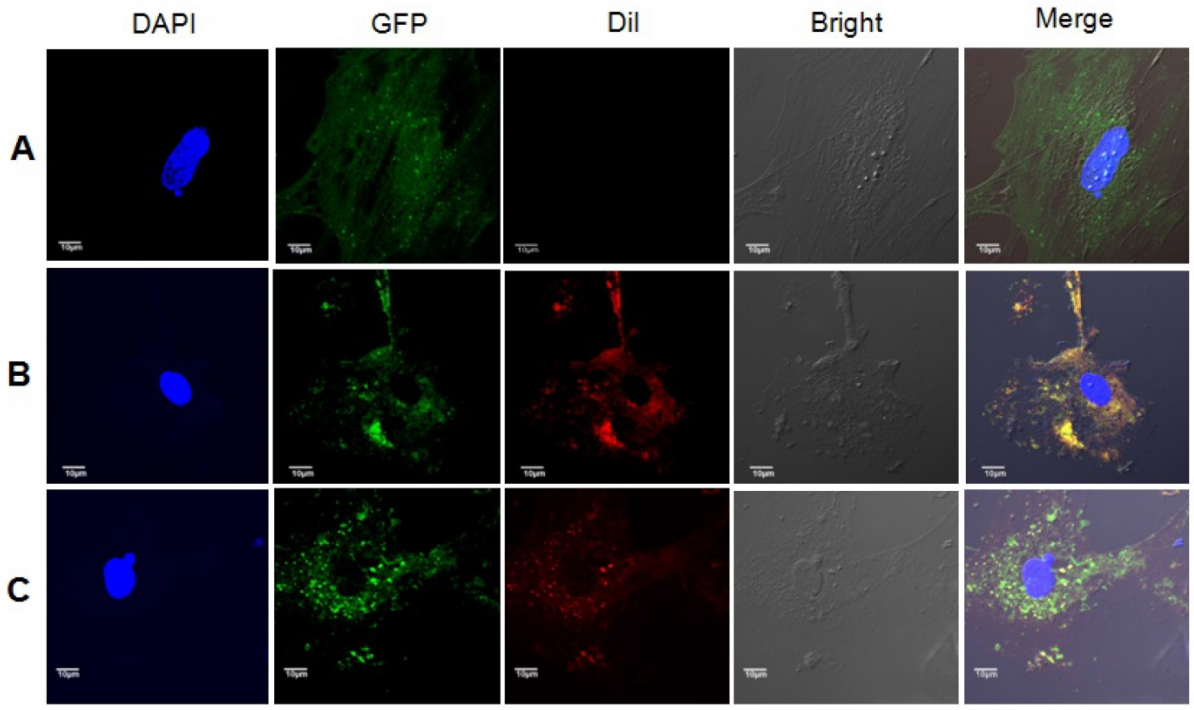


**Figure 6. Exosomes from irradiated astrocytes induced bystander autophagy *in vitro*.** Exosomes extracted from Panel A: sham irradiated astrocytes without Dil staining, Panel B: sham irradiated astrocytes with Dil staining, and Panel C: Exosomes from irradiated astrocytes were added into culture medium of non-irradiated primary astrocytes from LC3B-GFP transgenic mice. The recipients astrocytes were observed and pictured under confocal microscopy. Note. Red: exosomes stained with Dil; Green: LC3B-GFP; Blue: nuclei stained with DAPI (4',6-diamidino-2-phenylindole).

We next conducted animal study to further confirm our hypothesis. LC3B-GFP mice were injected with exosomes from irradiated or non-irradiated cells via their tail vein. The internalization of Dil-stained exosomes by lung cells, and the subsequently induction of autophagy in lung cells from mice injected with exosomes from irradiated astrocytes were observed under confocal microscopy (Fig. 7). Lung tissues were extracted after the injection of exosomes, and the qRT-PCR results showed increased miR-7 and decrease *Bcl-2* levels in mice injected with exosomes from irradiated astrocytes compared with control group (Fig. 8A). Consistenly, the western blotting results showed increased ratio of LC3B-II/LC3B-I, level of Beclin-1, and decreased level of BCL-2 in lung from irradiated group compared with control group (Fig. 8B).

## Discussion

RT is widely used as the major cancer treatment method, however, its genotoxic and carcinogenic nature means that strategies to protect and mitigate RT-induced normal tissue injury are required urgently. In the past two decades, increasing evidence has proved the existence of RIBE [4, 24, 25]. IR can induce detrimental biological effects, including carcinogenesis, in tissues and organs distant to radiation field. Thus, our traditional understanding of radiation biology has changed, and the protection of normal tissue from RT has become a challenge.

Recent evidence suggested that RIBE could be manifested in various forms, including autophagy [6, 9]. In the present study, we observed increasing expressions of autophagy markers in lungs after brain irradiation *in vivo*. Therefore, we assumed that autophagy could be used as a research endpoint for distant RIBE. In addition, no obvious induction of autophagy was detected in other organs, such as the spleen and small intestine. It is believed that in RIBE, the IR induced signal is transmitted by soluble factors in the circulatory system [2]; therefore, the reason that we detected RIBE in the lung instead of the spleen and small intestine might reflect the higher vascular density and blood flow velocity in the lung.

Some studies have already indicated the involvement of miRNAs in the cellular response to RIBE [6, 23, 26]; however, *in vivo* evidence still lacks. In the current study, we identified miR-7 as a potential mediator of lung bystander autophagy. We confirmed that after irradiation, miR-7 can be released by the brain into blood, then it transferred to the lung to trigger distant bystander autophagy. In one published paper, the authors found that miR-7 could suppress the proliferation of lung cancer cell by inhibiting *Bcl-2*, and they further proved that BCL-2 was downregulated by miR-7 at both transcriptional and translational levels [27], indicating that *Bcl-2* may

be directly targeted by miR-7. Consistent with that, our bioinformatics analysis and subsequently qRT-PCR identified that the autophagy-related gene *Bcl-2* was the target of miR-7. Thus, the results suggested that brain-released miR-7 mediates bystander lung autophagy by targeting *Bcl-2* upon brain irradiation.

Exosomes mediate communication between donator and recipient cells by transferring miRNAs, proteins and nucleic acids. During the "traveling" period, exosomes protect inside content from degradation. Once reach the "destination", exosomes are internalized and the contents inside are released into recipient cells [12, 13]. Recently exosomes-mediated transport has been implicated in several physiological and pathological processes. It is reported that cardiomyocytes-secreted exosome can enhance angiogenesis in recipient endothelial cells by transporting miRNA and proteins [28], indicating the involvement of exosomes-mediated transport in angiogenesis. In cancers, exosomes released by tumor cells can cause malignant alteration in recipient cells. For instance, exosome-mediated transport of αvβ3 integrin from prostate cancer cells can induce a migratory phenotype in nontumorigenic recipient cells [29]. Similarly, exosome-mediated transport of miR-9 from breast cancer cells could promote cancer-associated fibroblast-like properties in recipient normal fibroblasts [30]. Meanwhile, recently exosome-based transport system has been investigated to treat genetic neurodegenerative diseases by delivering miRNA or siRNA [31, 32]. Our and other lately published studies identified a role for exosomes in RIBE [6, 15], and we found that exosomal miR-7-5p secreted by irradiated cells induced autophagy in recipient non-irradiated bystander cells. Therefore, we hypothesized that exosomal miR-7 mediates bystander lung autophagy. The data suggested that exosomes derived from irradiated cells, which contain high levels of miR-7, were internalized and induced bystander autophagy in recipient cells. We then conducted *in vivo* studies to further verify this hypothesis. Consistent with the *in vitro* data, immunofluorescence confirmed the internalization of exosomes into the lung and subsequent induction of autophagy. QRT-PCR and western blotting showed increased miR-7 levels, decreased *Bcl-2* levels, and increased autophagy markers in the lungs of mice injected with exosomes from irradiated astrocytes. These data provided *in vivo* evidence that exosomes from irradiated cells were internalized and induced distant bystander autophagy in lung tissue via exosomal miR-7's effects on Bcl-2 signaling.

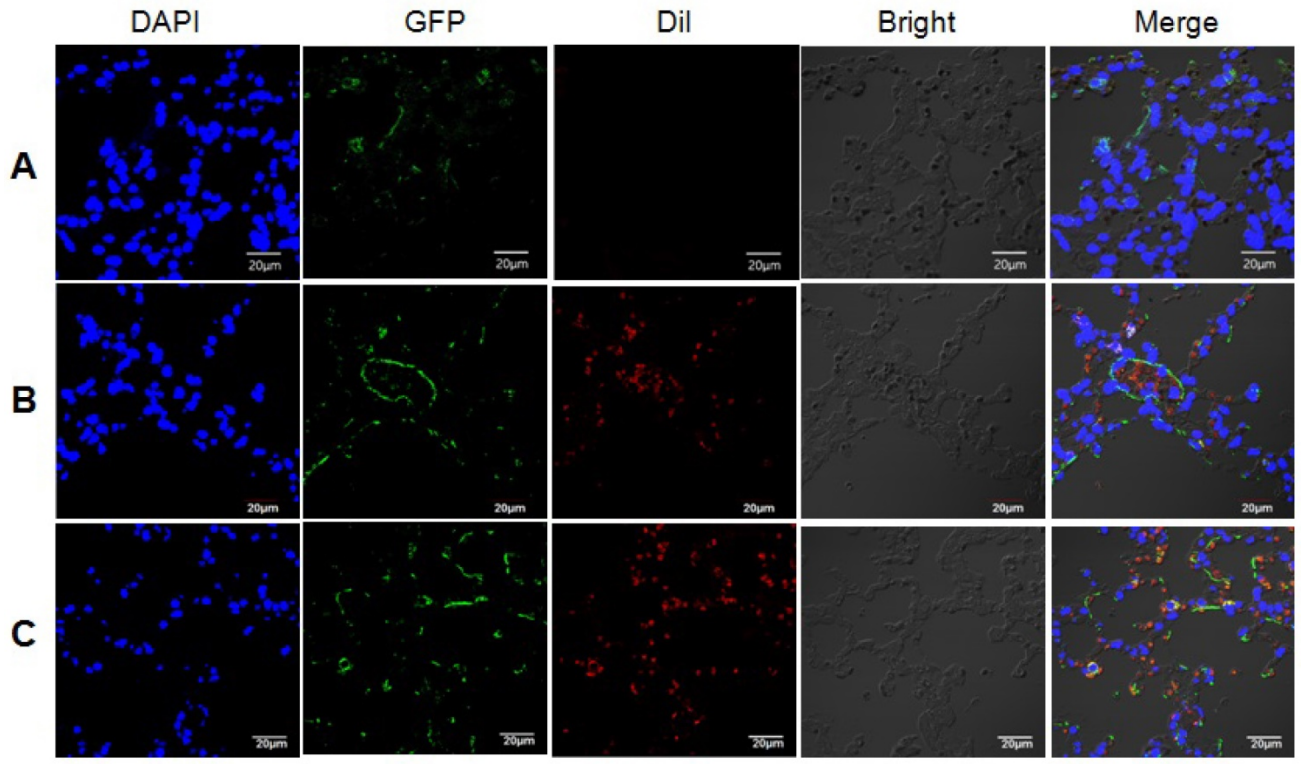


**Figure 7. Exosomes from irradiated astrocytes induced bystander autophagy *in vivo*.** Exosomes extracted from Panel A: sham irradiated astrocytes without DiI staining, and Panel B: sham irradiated astrocytes with DiI staining, Panel C: Exosomes from irradiated astrocytes were injected into LC3B-GFP transgenic mice via the tail vein several times. 6h after the last injection, mouse lung tissues were obtained and observed under confocal microscopy. Note. Red: exosomes stained with DiI; Green: LC3B-GFP; Blue: nuclei stained with DAPI (4',6-diamidino-2-phenylindole).

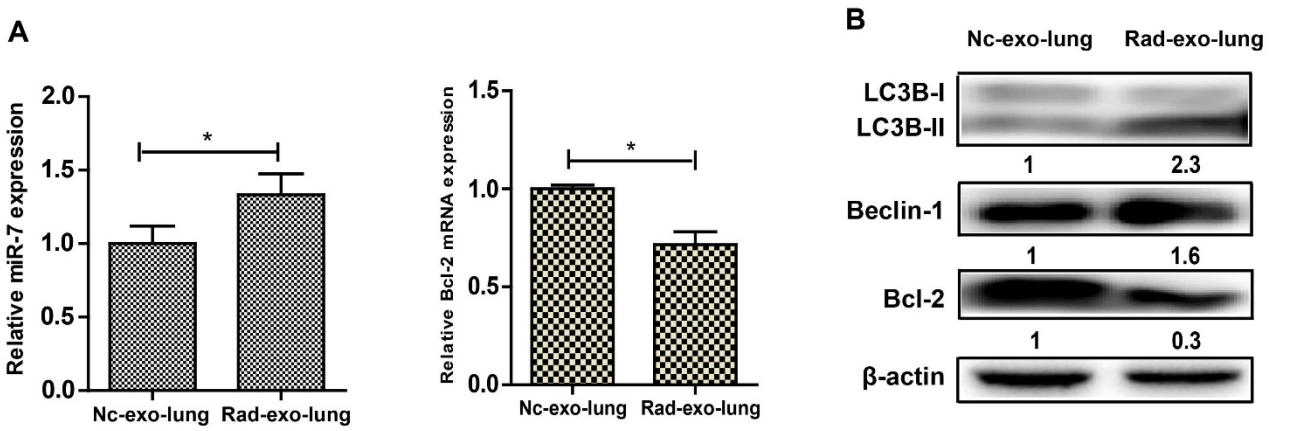


**Figure 8. Exosomal miR-7 mediates bystander autophagy *in vivo*.** After injected with irradiated (rad-exo) or non-irradiated (nc-exo) astrocytes-released exosomes, Panel A: Expression of miR-7 and *Bcl-2* mRNA in mice lung tissue were measured by qRT-PCR; U6 was used as internal control. Panel B: Expression of LC3B, Beclin-1, and Bcl-2 in mice lung tissue were measured by western blotting. Bars represent the mean ± SD, n=5, * *P* value < 0.05.

In summary, our study found that irradiation of mouse brain induced distant bystander lung autophagy, in which *Bcl-2* is a direct target of miR-7. For the first time, our *in vitro* and *in vivo* results confirmed that exosomal miR-7 mediates the distant bystander lung autophagy via Bcl-2. These results could form the basis for further research into the molecular mechanism of RIBE, and might help develop better strategies to protect normal tissue from RT-induced injury.

## Acknowledgements

This work was supported by the Chinese National Natural Science Foundation (Grant 81573077) and the project funded by the Priority Academic Program Development of Jiangsu Higher Education Institutions (PAPD).

## Competing Interests

The authors have declared that no competing interest exists.

## References

1. Berkey FJ. Managing the adverse effects of radiation therapy. Am Fam Physician. 2010; 82(4): 381-8.
2. Mothersill C, Seymour CB. Cell-cell contact during gamma irradiation is not required to induce a bystander effect in normal human keratinocytes: Evidence for release during irradiation of a signal controlling survival into the medium. Radiat Res. 1998; 149: 256-62.
3. Mancuso M, Pasquali E, Leonardi S, et al. Oncogenic bystander radiation effects in Patched heterozygous mouse cerebellum. Proc Natl Acad Sci USA. 2008; 105: 12445-50.
4. Mancuso M, Giardullo P, Leonardi S, et al. Dose and spatial effects in long-distance radiation signaling in vivo: implications for abscopal tumorigenesis. Int J Radiat Oncol Biol Phys. 2013; 85: 813-9.
5. Aravindan S, Natarajan M, Ramraj SK, et al. Abscopal effect of low-let gamma-radiation mediated through rel protein signal transduction in a mouse model of nontargeted radiation response. Cancer Gene Ther. 2014; 21: 54-9.
6. Song M, Wang Y, Shang ZF, et al. Bystander autophagy mediated by radiation-induced exosomal miR-7-5p in non-targeted human bronchial epithelial cells. Sci Rep. 2016; 6: 30165.
7. Zhong Z, Sanchez-Lopez E, Karin M. Autophagy, Inflammation, and Immunity: A Troika Governing Cancer and Its Treatment. Cell. 2016; 166: 288-98.
8. Zois CE, Koukourakis MI. Radiation-induced autophagy in normal and cancer cells: towards novel cytoprotection and radio-sensitization policies? Autophagy. 2009; 5: 442-50.
9. Wang X, Zhang J, Fu J, et al. Role of ROS-mediated autophagy in radiation-induced bystander effect of hepatoma cells. Int J Radiat Biol. 2015; 91: 452-8.
10. Keerthikumar S, Chisanga D, Ariyaratne D, et al. ExoCarta: A Web-Based Compendium of Exosomal Cargo. J Mol Biol. 2016; 428: 688-92.
11. Kowal J, Tkach M, Thery C. Biogenesis and secretion of exosomes. Curr Opin Cell Biol. 2014; 29: 116-25.
12. Tian T, Zhu YL, Hu FH, et al. Dynamics of exosome internalization and trafficking. J Cell Physiol. 2013; 228: 1487-95.
13. Valadi H, Ekstrom K, Bossios A, et al. Exosome-mediated transfer of mRNAs and microRNAs is a novel mechanism of genetic exchange between cells. Nat Cell Biol. 2007; 9: 654-9.
14. Jelonek K, Widlak P, Pietrowska M. The Influence of Ionizing Radiation on Exosome Composition, Secretion and Intercellular Communication. Protein Pept Lett. 2016; 23: 656-63.
15. Al-Mayah A, Bright S, Chapman K, et al. The non-targeted effects of radiation are perpetuated by exosomes. Mutat Res. 2015; 772: 38-45.
16. Bartel DP. MicroRNAs: genomics, biogenesis, mechanism, and function. Cell. 2004; 116: 281-97.
17. Li Z, Yu X, Shen J, et al. MicroRNA in intervertebral disc degeneration. Cell Prolif. 2015; 48: 278-83.
18. Li Z, Yu X, Shen J, et al. MicroRNA expression and its implications for diagnosis and therapy of gallbladder cancer. Oncotarget. 2015; 6: 13914-21.
19. Yu X, Li Z. The role of microRNAs expression in laryngeal cancer. Oncotarget. 2015; 6: 23297-305.
20. Li Z, Yu X, Shen J, et al. MicroRNA dysregulation in uveal melanoma: a new player enters the game. Oncotarget. 2015; 6: 4562-8.
21. Zhang S, Wang W, Gu Q, et al. Protein and miRNA profiling of radiation-induced skin injury in rats: the protective role of peroxiredoxin-6 against ionizing radiation. Free Radic Biol Med. 2014; 69: 96-107.
22. Lu J, Chen C, Hao L, et al. MiRNA expression profile of ionizing radiation-induced liver injury in mouse using deep sequencing. Cell Biol Int. 2016; 40: 873-86.
23. Xu S, Ding N, Pei H, et al. MiR-21 is involved in radiation-induced bystander effects. RNA Biol. 2014; 11: 1161-70.
24. Nagasawa H, Little JB. Induction of sister chromatid exchanges by extremely low doses of alpha-particles. Cancer Res. 1992; 52: 6394-6.
25. Huang L, Kim PM, Nickoloff JA, et al. Targeted and nontargeted effects of low-dose ionizing radiation on delayed genomic instability in human cells. Cancer Res. 2007; 67: 1099-104.
26. Dickey JS, Zemp FJ, Martin OA, et al. The role of miRNA in the direct and indirect effects of ionizing radiation. Radiat Environ Biophys. 2011; 50: 491-9.
27. Xiong S, Zheng Y, Jiang P, et al. MicroRNA-7 inhibits the growth of human non-small cell lung cancer A549 cells through targeting BCL-2. Int J Biol Sci. 2011; 7(6): 805-14.
28. Garcia NA, Ontoria-Oviedo I, González-King H, et al. Glucose Starvation in Cardiomyocytes Enhances Exosome Secretion and Promotes Angiogenesis in Endothelial Cells. PLoS One. 2015; 10(9): e0138849.
29. Singh A, Fedele C, Lu H, et al. Exosome-mediated Transfer of alphavbeta3 Integrin from Tumorigenic to Nontumorigenic Cells Promotes a Migratory Phenotype. Mol Cancer Res. 2016; 14(11): 1136-46.
30. Baroni S, Romero-Cordoba S, Plantamura I, et al. Exosome-mediated delivery of miR-9 induces cancer-associated fibroblast-like properties in human breast fibroblasts. Cell Death Dis. 2016; 7(7): e2312.
31. Lee ST, Im W, Ban JJ, et al. Exosome-Based Delivery of miR-124 in a Huntington's Disease Model. J Mov Disord. 2017; 10(1): 45-52.
32. Didiot MC, Hall LM, Coles AH, et al. Exosome-mediated Delivery of Hydrophobically Modified siRNA for Huntingtin mRNA Silencing. Mol Ther. 2016; 24(10): 1836-47.